

Local-field effects in NiO and Ni

F. Aryasetiawan and O. Gunnarsson

Max-Planck-Institut für Festkörperforschung, D-70506 Stuttgart, Germany

M. Knupfer and J. Fink

Institut für Festkörperforschung, IFW Dresden e.V., D-01171 Dresden, Germany

(Received 22 March 1994)

We have calculated the electron energy-loss function for NiO and Ni using the random phase approximation. Experimental results are presented for NiO, and it is shown that theory is in rather good agreement with experiment. The local-field effects are shown to be small for the loss function, although the system is very inhomogeneous, while they are large for the static dielectric function. We demonstrate that the size of the local-field effects are governed by a certain Coulomb integral w which is determined by the important transitions. These are $3d \rightarrow 4f$ transitions for the loss function, where w_{df} is small, and $3d \rightarrow 3d$ and $4s \rightarrow 4s$ for the static dielectric function, where w_{dd} is large. We discuss how the local-field effects reduce the static screening. We show that this reduction is so efficient for the $3d \rightarrow 3d$ contribution that the $4s \rightarrow 4s$ contribution plays a substantial role for the static dielectric function, although the $4s$ density of states is much smaller than the $3d$ density of states.

I. INTRODUCTION

NiO has attracted much interest as a widely studied example of an insulator, where the gap is primarily due to many-body effects.¹⁻³ Thus it is found that in the local density approximation (LDA) of the density functional formalism,⁴ the band gap is very small (at the most a few tenths of an eV),⁵ while the experimental gap is large (~ 4 eV).^{3,6} Here we calculated the dielectric function $\epsilon(\mathbf{q}, \omega)$ and the loss function $\text{Im } 1/\epsilon(\mathbf{q}, \omega)$ for NiO and Ni using the random-phase approximation⁷⁻⁹ (RPA) together with the LDA band structure and compare with experimental result for the loss function, obtained from electron energy-loss spectroscopy (EELS) for NiO.

While it is clear that this approach leads to incorrect results for low energies ($\omega \leq 4$ eV) due to the incorrect LDA band gap, it is interesting to see how good the description is over a larger energy range ($\omega \geq 4$ eV), where almost all the weight of $\text{Im } 1/\epsilon(\mathbf{q}, \omega)$ is located. This quantity is particularly interesting, since $\text{Im } \epsilon^{-1}(\mathbf{q}, \omega)$ is an important input in many-body calculations, which attempt to improve on the poor band gap in the LDA, such as the so-called *GW* method,^{10,11} in which the lowest-order self-energy is calculated. Below we show that a satisfactory description of $\text{Im } 1/\epsilon(\mathbf{q}, \omega)$ is obtained for $\omega \geq 4$ eV, although the quality is not quite as good as for Ni metal.¹²

Another interesting aspect of NiO are the local-field effects. In the RPA one calculates the response of non-interacting electrons to an effective field consisting of the external field and the field from the induced charge. Since the system is inhomogeneous, the induced charge has rapid spatial variations, even when the external field is slowly varying. In the simplest approach one averages out these rapid variations and only keeps the same Fourier components as for the external field. We refer to

the corresponding dielectric function as ϵ_{NLF} (nonlocal-field), while the one which includes the effects of the rapid variations (local-field effects) is called ϵ_{LF} .

The importance of the local-field effects is expected to increase with increasing inhomogeneity of the system. It is well known that there are substantial local-field effects for semiconductors, such as Si.¹³ Since NiO is substantially more inhomogeneous, one may expect the effects to be even larger. We find that the local-field effects indeed are large for the static dielectric function. For the loss function, $\text{Im } 1/\epsilon(\mathbf{q}, \omega)$ with ω large and $|\mathbf{q}|$ small, we find, however, that the effects are small.

We discuss these surprising results in detail. Since similar results are also found for Ni metal, we focus in the discussion on this simpler system. We consider the dominant transitions, which are of $3d$ - $3d$ type for the static dielectric function and of $3d$ - $4f$ type for the loss function. We show that the local-field effects are related to the magnitude of a Coulomb integral w for a charge density $\rho_\mu(\mathbf{r}) - \bar{\rho}$, where $\rho_\mu(\mathbf{r})$ is the product of the two functions involved in the most important transition and $\bar{\rho}$ is the average of this product. Since the $3d$ orbital is very peaked, the corresponding charge density takes large values, even after its average has been subtracted, leading to a large Coulomb integral w (~ 9 eV) and explaining the importance of the local-field effects for the static dielectric function. The product of a $3d$ and a $4f$ function, on the other hand, has a much smoother behavior, since the $3d$ function is peaked in the inner part of the atom while the $4f$ function is peaked further out. As a result its amplitude has a rather modest variation and is relatively small everywhere. The corresponding Coulomb integral w is very small (~ 0.2 eV), explaining the small local-field effects for the loss function.

In the case of the static dielectric function for Ni, we find that the local-field effects reduce the efficiency of

the 3d electron screening so much that the 4s and 4p electrons also become important for the screening. To illustrate these effects we present two simple models with one or two important transitions, respectively.

In the RPA, we only consider the response of the electrons to the Hartree potential. In addition, however, the electrons feel changes in the exchange-correlation (XC) potential, induced by changes in the density. These XC effects are also often referred to as local-field effects, and appear already for a homogeneous system. We refer to these local-field effects as XC local-field effects, while the local-field effects due to the inhomogeneity of the system we refer to as simply local-field effects. In this paper, we focus on the latter, but we also give a brief discussion of the XC local-field effects.

In Sec. II, we present the formalism for the dielectric function and in Sec. III, we present computational and experimental details. In Sec. IV, we compare theory and experiment for NiO and in Sec. V, we discuss the local-field effects in terms of two model calculations. The XC local-field effects are discussed in Sec. VI and the summary is given in Sec. VII.

II. DIELECTRIC FUNCTION

In this section, we discuss the general formalism for calculating the dielectric function. The irreducible polarizability for the frequency ω in the RPA is given by⁷⁻⁹

$$P^0(\mathbf{r}, \mathbf{r}'; \omega) = 2 \sum_{\mathbf{k}n}^{\text{occ}} \sum_{\mathbf{k}'n'}^{\text{unocc}} \psi_{\mathbf{k}n}^*(\mathbf{r}) \psi_{\mathbf{k}'n'}(\mathbf{r}) \psi_{\mathbf{k}'n'}^*(\mathbf{r}') \psi_{\mathbf{k}n}(\mathbf{r}') \times \left\{ \frac{1}{\omega - \epsilon_{\mathbf{k}'n'} + \epsilon_{\mathbf{k}n} + i\delta} - \frac{1}{\omega + \epsilon_{\mathbf{k}'n'} - \epsilon_{\mathbf{k}n} - i\delta} \right\}, \quad (1)$$

where $\psi_{\mathbf{k}n}(\mathbf{r})$ is the wave function for a state with the wave vector \mathbf{k} , band index n , and energy $\epsilon(\mathbf{k}n)$. The wave function is normalized to unity in the entire space and the factor 2 comes from summation over spin. The Bloch states $\psi_{\mathbf{k}n}(\mathbf{r})$ are expressed as

$$\psi_{\mathbf{k}n}(\mathbf{r}) = \sum_{\mathbf{R}L} \chi_{\mathbf{R}L}(\mathbf{r}, \mathbf{k}) b_{\mathbf{R}L}(\mathbf{k}n), \quad (2)$$

with

$$\chi_{\mathbf{R}L}(\mathbf{r}, \mathbf{k}) = \frac{1}{\sqrt{N}} \sum_{\mathbf{T}} e^{i\mathbf{k}\cdot\mathbf{T}} \chi_{\mathbf{R}L}(\mathbf{r} - \mathbf{R} - \mathbf{T}), \quad (3)$$

where N is the number of cells and \mathbf{R} gives the positions of the atoms inside the unit cell relative to the position \mathbf{T} of the unit cell. $\chi_{\mathbf{R}L}$ is the basis function on a given atom centered at \mathbf{R} with angular momentum $L \equiv lm$. It is possible to have multiple orbitals with different energies for a given L ,¹⁴ but for simplicity we consider only one orbital per L channel. In the linear-muffin-tin-orbital (LMTO) method used below, and within the atomic sphere ap-

proximation, where the space is filled with spheres, $\chi_{\mathbf{R}L}$ has the following form:¹⁵

$$\chi_{\mathbf{R}L} = \phi_{\mathbf{R}L} + \sum_{\mathbf{R}'L'} \dot{\phi}_{\mathbf{R}'L'} h_{\mathbf{R}'L', \mathbf{R}L}, \quad (4)$$

$\phi_{\mathbf{R}L}$ is a solution to the radial Schrödinger equation inside a sphere centered at \mathbf{R} at an energy ϵ_ν , chosen at the center of the band of interest, and $\dot{\phi}_{\mathbf{R}L}$ is its energy derivative. $\phi_{\mathbf{R}L}$ and $\dot{\phi}_{\mathbf{R}L}$ are only defined inside a sphere centered at \mathbf{R} . From Eq. (4), it is clear that $\psi_{\mathbf{k}n}(\mathbf{r}) \psi_{\mathbf{k}'n'}(\mathbf{r})$ consists of products of the type $\phi\phi$, $\phi\dot{\phi}$, and $\dot{\phi}\dot{\phi}$, each localized in its sphere and zero outside. We, therefore, introduce a new product basis set^{16,17} for describing the polarizability

$$\tilde{B}_\mu(\mathbf{r}) \equiv \tilde{\phi}_{\mathbf{R}L}(\mathbf{r}) \tilde{\phi}_{\mathbf{R}'L'}(\mathbf{r}); \mu = (\mathbf{R}L, L'), \quad (5)$$

where $\tilde{\phi}$ can be either ϕ or $\dot{\phi}$. This product basis is complete for P^0 by construction and the response function may be expanded in this basis as follows:

$$P^0(\mathbf{r}, \mathbf{r}', \omega) = \sum_{\mathbf{q}} \sum_{\mu\nu} \tilde{B}_{\mathbf{q}\mu}(\mathbf{r}) \tilde{P}_{\mu\nu}^0(\mathbf{q}, \omega) \tilde{B}_{\mathbf{q}\nu}^*(\mathbf{r}'), \quad (6)$$

where $\tilde{B}_{\mathbf{q}\mu}$ is a Bloch sum of \tilde{B}_μ as in Eq. (3). The sum over \mathbf{q} is limited to the first Brillouin zone and

$$\tilde{P}_{\mu\nu}^0(\mathbf{q}, \omega) = \frac{2}{N} \sum_{\mathbf{k}n}^{\text{occ}} \sum_{\mathbf{n}'}^{\text{unocc}} \tilde{b}_{\mathbf{R}L_1}(\mathbf{k}n) \tilde{b}_{\mathbf{R}L_2}^*(\mathbf{k} + \mathbf{q}n') \times \tilde{b}_{\mathbf{R}'L_3}^*(\mathbf{k}n) \tilde{b}_{\mathbf{R}'L_4}(\mathbf{k} + \mathbf{q}n') \times \left\{ \frac{1}{\omega - \epsilon_{\mathbf{k} + \mathbf{q}n'} + \epsilon_{\mathbf{k}n} + i\delta} - \frac{1}{\omega + \epsilon_{\mathbf{k} + \mathbf{q}n'} - \epsilon_{\mathbf{k}n} - i\delta} \right\}, \quad (7)$$

with $\mu = \mathbf{R}L_1, L_2$ and $\nu = \mathbf{R}'L_3, L_4$. The quantity \tilde{b} is defined as $\tilde{b} = b$ or $\tilde{b} = hb$ depending on the meaning of \tilde{B} . Here the $\tilde{}$ indicates that \tilde{P}^0 is expressed in the basis states $\tilde{B}_{\mathbf{q}\mu}$. In this way we have expressed the irreducible polarizability in terms of matrices with the dimension $M = 3n_a \{N_v(N_v + 1)/2 + N_c N_v\}$, where n_a is the number of atoms per unit cell, $N_v = l_{\text{max}}(l_{\text{max}} + 1)$ and N_c are the number of valence and core states per atom, respectively, and l_{max} is the maximum l quantum number used. In the actual calculations, the dimension of this matrix is considerably reduced by neglecting product functions containing $\dot{\phi}$ and contracting the basis to optimized linear combinations of the states in Eq. (5).¹⁷

We now consider the screening of an external potential

$$V^{\text{ext}}(\mathbf{r}, t) = V^{\text{ext}}(\mathbf{r}, \omega) e^{-i\omega t} = V^{\text{ext}}(\mathbf{q}, \omega) e^{i(\mathbf{q}\cdot\mathbf{r} - \omega t)} / \sqrt{N\Omega}, \quad (8)$$

where Ω is the volume of the unit cell. The screened potential, $V^{\text{scr}}(\mathbf{r}, \omega)$, satisfies the equation

$$V^{\text{scr}}(\mathbf{r}, \omega) = V^{\text{ext}}(\mathbf{r}, \omega) + \int d^3r' \int d^3r'' \times v(\mathbf{r} - \mathbf{r}') P^0(\mathbf{r}', \mathbf{r}'', \omega) V^{\text{scr}}(\mathbf{r}'', \omega), \quad (9)$$

where $v(\mathbf{r} - \mathbf{r}')$ is the unscreened Coulomb interaction. This equation describes how the screened potential induces a charge density of the type $P^0 V^{\text{scr}}$, which gives rise to an induced potential $v P^0 V^{\text{scr}}$ which has to be added to the external potential. To solve for V^{scr} , we notice that due to the separable form^{16,18} of P_0 in Eq. (6), only integrals over $\tilde{B}_{\mathbf{q}\nu}^*(\mathbf{r}'') V^{\text{scr}}(\mathbf{r}'', \omega)$ enter in the second term of Eq. (9). Thus we introduce

$$\tilde{V}_{\mu}^{\text{scr}}(\mathbf{q}, \omega) = \int d^3 r \tilde{B}_{\mathbf{q}\mu}^*(\mathbf{r}) V^{\text{scr}}(\mathbf{r}, \omega), \quad (10)$$

together with a similar definition for \tilde{V}^{ext} . We then find

$$\begin{aligned} \tilde{V}_{\mu}^{\text{scr}}(\mathbf{q}, \omega) &= \tilde{V}_{\mu}^{\text{ext}}(\mathbf{q}, \omega) \\ &+ \sum_{\nu\lambda} \tilde{v}_{\mu\nu}(\mathbf{q}) \tilde{P}_{\nu\lambda}^0(\mathbf{q}, \omega) \tilde{V}_{\lambda}^{\text{scr}}(\mathbf{q}, \omega), \end{aligned} \quad (11)$$

where

$$\tilde{v}_{\mu\nu}(\mathbf{q}) = \int d^3 r d^3 r' \tilde{B}_{\mathbf{q}\mu}^*(\mathbf{r}) v(\mathbf{r} - \mathbf{r}') \tilde{B}_{\mathbf{q}\nu}(\mathbf{r}'). \quad (12)$$

This kind of Coulomb integral has also been used in the calculation of the Hartree-Fock energy.¹⁹ In a traditional treatment, the screened potential is Fourier transformed and represented by the Fourier coefficients corresponding to the wave vectors $\mathbf{q} + \mathbf{G}$, where \mathbf{G} is a reciprocal lattice vector. One then finds that the Fourier coefficient $V^{\text{scr}}(\mathbf{q} + \mathbf{G})$ influences the induced charge $\rho(\mathbf{q})$. Here we collect all the different Fourier coefficients in an appropriate way by considering the transform in Eq. (10), and we do not need to consider higher reciprocal lattice vectors explicitly.

We now treat v and P^0 as matrices and V^{ext} and V^{scr} as vectors with indices $\mu = \mathbf{R}L, L'$. The solution of Eq. (11) can be written as

$$\tilde{V}^{\text{scr}} = (1 - \tilde{v} \tilde{P}^0)^{-1} \tilde{V}^{\text{ext}}, \quad (13)$$

and using Eqs. (6) and (10) we obtain from Eq. (9)

$$\begin{aligned} V^{\text{scr}}(\mathbf{r}, \omega) &= V^{\text{ext}}(\mathbf{r}, \omega) + \int d^3 r' \sum_{\mathbf{q}\mu\nu} v(\mathbf{r} - \mathbf{r}') \\ &\times \tilde{B}_{\mathbf{q}\mu}(\mathbf{r}') \tilde{P}_{\mu\nu}^0(\mathbf{q}, \omega) \tilde{V}_{\nu}^{\text{scr}}(\mathbf{q}, \omega). \end{aligned} \quad (14)$$

To determine the dielectric function in the limit $\mathbf{q} \rightarrow 0$, we take the Fourier transform of Eq. (14), and denote the Fourier transforms of $V^{\text{scr}}(\mathbf{r}, \omega)$ and $V^{\text{ext}}(\mathbf{r}, \omega)$ by $V^{\text{scr}}(\mathbf{q}, \omega)$ and $V^{\text{ext}}(\mathbf{q}, \omega)$, respectively. We further write

$$\tilde{B}_{\mathbf{q}\mu}(\mathbf{r}) = \frac{1}{\sqrt{N\Omega}} \left\{ f_{\mu}(\mathbf{q}) e^{i\mathbf{q}\cdot\mathbf{r}} + \sum_{\mathbf{G} \neq 0} f_{\mu}(\mathbf{q} + \mathbf{G}) e^{i(\mathbf{q} + \mathbf{G})\cdot\mathbf{r}} \right\}, \quad (15)$$

where \mathbf{q} is limited to the first Brillouin zone. Here

$$f_{\mathbf{R}L L'}(\mathbf{q} \rightarrow 0) = \frac{\delta_{L, L'}}{\sqrt{\Omega}}. \quad (16)$$

Using Eq. (13) in Eq. (14) and the relation $\tilde{V}_{\nu}^{\text{ext}}(\mathbf{q}, \omega) =$

$f_{\nu}^*(\mathbf{q}) V^{\text{ext}}(\mathbf{q}, \omega)$, we obtain

$$\begin{aligned} V^{\text{scr}}(\mathbf{q}, \omega) &= V^{\text{ext}}(\mathbf{q}, \omega) \\ &+ v(\mathbf{q}) \sum_{\mu\nu} f_{\mu}(\mathbf{q}) \tilde{P}_{\mu\nu}(\mathbf{q}, \omega) f_{\nu}^*(\mathbf{q}) V^{\text{ext}}(\mathbf{q}, \omega), \end{aligned} \quad (17)$$

where $\tilde{P} = \tilde{P}^0(1 - \tilde{v} \tilde{P}^0)^{-1}$ and $v(\mathbf{q}) = 4\pi e^2/q^2$. The inverse dielectric function is given by

$$\begin{aligned} \epsilon_{\text{LF}}^{-1}(\mathbf{q}, \omega) &= \frac{V^{\text{scr}}(\mathbf{q}, \omega)}{V^{\text{ext}}(\mathbf{q}, \omega)} \\ &= 1 + v(\mathbf{q}) \sum_{\mu\nu} f_{\mu}(\mathbf{q}) \tilde{P}_{\mu\nu}(\mathbf{q}, \omega) f_{\nu}^*(\mathbf{q}) \\ &= 1 + v(\mathbf{q}) P(\mathbf{q}, \omega). \end{aligned} \quad (18)$$

This expression contains local-field effects. We now consider the matrix element $\tilde{v}_{\mu\nu}(\mathbf{q})$ in more detail. Thus we write

$$\tilde{v}_{\mu\nu}(\mathbf{q}) = f_{\mu}^*(\mathbf{q}) v(\mathbf{q}) f_{\nu}(\mathbf{q}) + w_{\mu\nu}(\mathbf{q}), \quad (19)$$

where

$$w_{\mu\nu}(\mathbf{q}) = \sum_{\mathbf{G} \neq 0} v(|\mathbf{q} + \mathbf{G}|) f_{\mu}^*(\mathbf{q} + \mathbf{G}) f_{\nu}(\mathbf{q} + \mathbf{G}). \quad (20)$$

From the definition (20) it is clear that $w_{\mu\mu}$ is obtained by constructing the charge density $\tilde{B}_{\mathbf{q}\mu}(\mathbf{r})$, subtracting the \mathbf{q} th Fourier component and then calculating the interaction of this charge density with itself. In the limit $\mathbf{q} \rightarrow 0$, which is the interesting limit here, a constant density is subtracted so that the resulting density integrates to zero. If the charge density $\tilde{B}_{\mathbf{q}\mu}(\mathbf{r})$ is relatively constant, the subtraction of the average charge leads to a small charge density, and $w_{\mu\mu}$ is correspondingly small, while for a $\tilde{B}_{\mathbf{q}\mu}(\mathbf{r})$ with a strong spatial variation, the subtraction of its average has a smaller effect and the corresponding $w_{\mu\mu}$ is large.

If we neglect all Fourier components of the induced charge density different from the Fourier component \mathbf{q} of the external potential, i.e., neglect the components $\mathbf{G} \neq 0$ in Eq. (15), we obtain that $w_{\mu\nu} = 0$. Using Eq. (11), this leads to

$$\begin{aligned} \epsilon_{\text{NLF}}(\mathbf{q}, \omega) &= 1 - v(\mathbf{q}) \sum_{\mu\nu} f_{\mu}(\mathbf{q}) \tilde{P}_{\mu\nu}^0(\mathbf{q}, \omega) f_{\nu}^*(\mathbf{q}) \\ &= 1 - v(\mathbf{q}) P^0(\mathbf{q}, \omega), \end{aligned} \quad (21)$$

where ϵ_{NLF} is the dielectric function without local-field corrections.

III. COMPUTATIONAL AND EXPERIMENTAL METHODS

We have performed calculations using a modified version of the linear-muffin-tin-orbital method,¹⁵ where we allow for several orbitals per l and m quantum number,¹⁷ where l and m are the angular and azimuthal quantum

numbers, respectively. The introduction of several orbitals per l and m may be necessary if we want to describe $\text{Im } \epsilon^{-1}(\mathbf{q}, \omega)$ over a large energy range $\hbar\omega \geq 1$ hartree, while otherwise it is sufficient to use one orbital per l and m . For energies of the order $\hbar\omega \geq 1$ hartree $4d$ functions become important, while higher functions for $l \neq 2$ enter only at substantially larger energies. To reduce the size of the matrices describing the dielectric function we have introduced basis states,¹⁷ which are linear combinations of the states $\tilde{B}_\mu(\mathbf{r})$ in Eq. (5). These linear combinations are optimized so that for a given number of such linear combination, the space of all functions $\tilde{B}_\mu(\mathbf{r})$ is spanned as completely as possible.

To simplify the integrations over the Brillouin zone in expressions of the type (7), we calculate the imaginary part and then obtain the real part from the Kramer-Kronig formula. The δ functions appearing in the imaginary part are replaced by

$$\delta(\epsilon) \rightarrow \frac{1}{\sigma\sqrt{\pi}} e^{-(\epsilon^2/\sigma^2)}, \quad (22)$$

where $\sigma = 0.05$ hartree has been used. Due to this smoothing of the δ function, the density of states obtained for Ni is smaller than is normally given, since the density of states varies very rapidly at the Fermi energy. For the qualitative discussion this is, however, not important. We observe, however, that the peak height in the loss function is rather sensitive to whether a Gaussian or Lorentzian is used to approximate the δ function.

In the calculations we introduce spheres around each atom, in such a way that the volumes of these atomic spheres add up to the volume of the unit cell (volume conservation). These spheres, therefore, overlap somewhat. In NiO we have introduced additional interstitial spheres, which are located between the atoms. The volume conservation then requires smaller spheres and the overlap between the spheres is reduced. There are two empty spheres per unit cell (with one NiO unit per unit cell), located at $(1,1,1)a/4$ and $(-1,-1,-1)a/4$, where a is the lattice constant. For Ni metal, we have in a similar way introduced one empty sphere per unit cell, located at $(1,1,1)a/2$. The functions $\phi_{\mathbf{R}L}(\mathbf{r})$ and their energy derivatives $\dot{\phi}_{\mathbf{R}L}(\mathbf{r})$ in Eq. (4) are defined inside such a sphere and put equal to zero outside.

To simplify the calculations for NiO we have considered a paramagnetic system instead of an antiferromagnetic system, which leads to a reduction of the unit cell from four atoms to two atoms per unit cell. This changes the results over a small energy scale only. In separate publications, we discuss the approximations and the tests we have performed in detail.^{14,17}

Experimentally, the loss function of NiO has been determined with EELS in transmission using a 170 keV spectrometer described elsewhere.²⁰ The energy and momentum resolutions were set to 150 meV and 0.05 \AA^{-1} , respectively. Thin films of about 1000-\AA thickness were cut from a NiO single crystal by an ultramicrotome with a diamond knife. Subsequently, the films were floated on electron-microscope grids and transferred into the spectrometer. Prior to the investigation of the loss function,

the samples were characterized by measuring the elastic electron diffraction spectrum. To obtain the loss function, the raw data have been corrected for the contribution of the elastic line and multiple losses²¹ after the measurements. The EELS studies were performed with a momentum transfer of 0.5 \AA^{-1} , in order to compare them to the theoretical results.

IV. RESULTS

In Fig. 1, we show $\text{Im } \epsilon_{\text{LF}}^{-1}(\mathbf{q}, \omega)$ for NiO, calculated according to Eq. (18), i.e., including local-field effects. We have considered a small value of $|\mathbf{q}|$ [$\mathbf{q} = (0.25, 0.00, 0.00)2\pi/a$], where $a = 7.899 a_0$ is the lattice parameter. The dashed curve shows results using one orbital per l and m quantum number, while the full curve was obtained using both $3d$ and $4d$ orbitals. We can see that for $\hbar\omega \leq 20$ eV, it is sufficient to use one orbital per l and m quantum number.

In Fig. 2, we compare calculations with (full line) and without (dashed line) local-field effects with experimental results. First of all we observe that there is an overall satisfactory agreement between theory and experiment. The main structure is the plasmon peak at about 24 eV, which is fairly well reproduced in terms of energy and weight, although the theoretical peak is too narrow. Also for other energies the intensity is rather well reproduced. For energies below about 4 eV there is no intensity according to experiment, while LDA gives intensity in this energy range, due to the incorrect band gap in the LDA. The theoretical intensity in this region is, however, very small. The theoretical curve also exaggerates some of the structures in the experimental results. For instance, there is a peak at about 9 eV in the calculation but only a shoulder experimentally. Also at 35–40 eV the calculation shows too much structure. Also earlier calculations, neglecting local-field effects, have found that the theoretical results are more structured and have narrower peaks

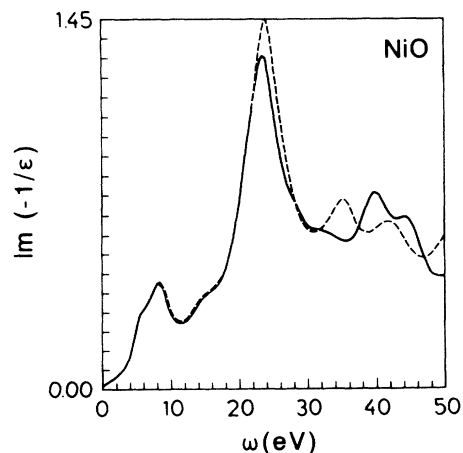


FIG. 1. The loss function $\text{Im } \epsilon^{-1}(\mathbf{q}, \omega)$ for NiO for $\mathbf{q} = (0.25, 0.00, 0.00)2\pi/a$. The full curve shows results obtained with one orbital per l and m quantum number and the dashed curve shows results when the Ni $4d$ orbital is included.

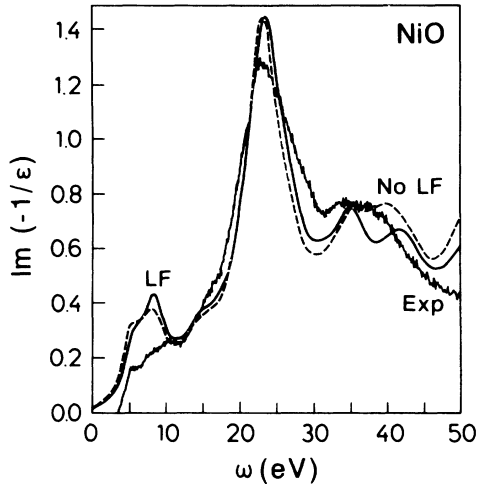


FIG. 2. Theoretical and experimental results for the loss function $\text{Im } \epsilon^{-1}(\mathbf{q}, \omega)$ for NiO. The (smooth) full and dashed curves show theoretical results with and without local-field effects, respectively, for $\mathbf{q} = (0.25, 0.00, 0.00)2\pi/a = 0.37 \text{ \AA}^{-1}$. The experimental results were measured at the momentum transfer of $|\mathbf{q}| = 0.5 \text{ \AA}^{-1}$. Since the absolute magnitude of the experimental results is not known, they have been normalized to the theoretical curves. The Ni 4d orbital is included in the calculations.

than the experimental results.²² A reason may be the lifetime broadening effects not included in the RPA.²² Nevertheless, the calculated results appear to be sufficiently accurate to provide a basis for the interpretation of the experimental results and as an input for many-body calculations.

We notice that the difference between the results with and without local-field effects is rather small. This is surprising, since NiO is a very inhomogeneous system, and one would expect the local-field effects to be large. Indeed, we find that for the static dielectric function, $\epsilon(\mathbf{q}, \omega = 0)$ there is a large difference. Thus we find that for $\mathbf{q} = (0.25, 0.00, 0.00)2\pi/a$ the dielectric function is 42 without and 20 with local-field effects, i.e., the difference is a factor of 2. This large difference in the importance of the local-field effects for the static dielectric function and the loss function will be discussed in detail in Sec. V.

Qualitatively similar results have been obtained for Ni metal.¹² In Fig. 3, we show results using the present formalism for Ni with (full line) and without (empty circles) local-field effects. As for NiO we can see that the differences between the two calculations are small. There are also appreciable similarities with the results for NiO. For instance, the plasmon peak is at about the same energy and has a comparable weight. A further similarity with NiO is that for the static dielectric function there is a large difference between the calculations with and without local-field corrections. For $\mathbf{q} = (0.25, 0.00, 0.00)2\pi/a$, we find that the static dielectric function is 23 and 68 with and without local-field corrections, respectively.

Because of the substantial similarities between NiO and Ni, we discuss below the effects of local-field cor-

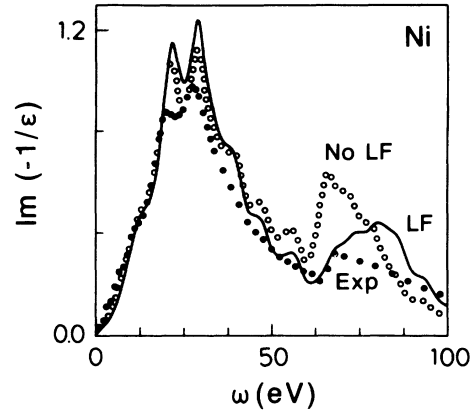


FIG. 3. The loss function $\text{Im } \epsilon^{-1}(\mathbf{q}, \omega)$ for Ni for $\mathbf{q} = (0.25, 0.00, 0.00)2\pi/a$. The full curve and empty circles show results with and without local-field effects, respectively, and the dotted curve shows experimental results (Ref. 23). The Ni 4d orbital is included in the calculations.

rections for Ni, which is simpler than NiO in the sense that Ni has only one atom per unit cell.

V. LOCAL-FIELD EFFECTS

In this section, we discuss in detail for Ni metal why the local-field effects are important for the static dielectric function but not for the loss function.

A. Static dielectric function

We consider the static case ($\omega = 0$) for small values of \mathbf{q} . In this limit the intraband transitions give the dominating contribution to \bar{P}^0 . The number of possible transitions goes to zero with $|\mathbf{q}|$, but the corresponding energy denominator also goes to zero, leading to a finite result, where \bar{P}^0 is determined by the partial densities of states. Because of the large 3d density of states, the 3d-3d transitions, therefore, play a dominating role for the dielectric function without local-field corrections. We have calculated the dielectric function by only including states $\bar{B}_{\mathbf{q}\mu}$ in Eq. (5) where μ stands for a product of two 3d functions, using the band structure calculated with the full basis set. We then obtain $\epsilon_{\text{NLF}} = 118$, in qualitative agreement with the full calculation, which gives $\epsilon_{\text{NLF}} = 68$. The smaller value in the full calculation is due to a partial cancellation by the off-diagonal terms in Eq. (6). With local-field corrections included, we obtain $\epsilon_{\text{LF}} = 10$ with only products of 3d functions, while the full calculation gives $\epsilon_{\text{LF}} = 23$. To improve the agreement, we also have to include a product of extended functions. For instance, using a product of two 4s functions in addition to the product of two 3d functions, we obtain $\epsilon_{\text{NLF}} = 72$ and $\epsilon_{\text{LF}} = 19$, in good agreement with the full calculation ($\epsilon_{\text{NLF}} = 68$ and $\epsilon_{\text{LF}} = 23$). To obtain a better understanding of these results, we consider a two-band model below where only one product of 4s

functions and one product of $3d$ functions are included, as well as a model with only one product of $3d$ functions.

For simplicity, we first consider a model with just one product basis state $\tilde{B}_{\mathbf{q}\mu}(\mathbf{r})$. This may refer to a product of two $3d$ functions in the case of the static dielectric function, or to the product of a $3d$ and a $4f$ function for the loss function, as discussed below. From Eq. (18) it follows that the dielectric function is

$$\epsilon_{\text{LF}}(\mathbf{q}, \omega) = 1 - \frac{v(q)|f(\mathbf{q})|^2 \tilde{P}^0(\mathbf{q}, \omega)}{1 - w(\mathbf{q})\tilde{P}^0(\mathbf{q}, \omega)}, \quad (23)$$

if local-field effects are included and

$$\epsilon_{\text{NLF}}(\mathbf{q}, \omega) = 1 - v(q)|f(\mathbf{q})|^2 \tilde{P}^0(\mathbf{q}, \omega), \quad (24)$$

if local-field effects are neglected. We can see that the local-field effects are important if $w(\mathbf{q})|\tilde{P}^0(\mathbf{q}, \omega)|$ is of the order one or larger. In Fig. 4 we show the product of two $3d$ radial functions. It is immediately clear that this product is very peaked for $r \sim 0.3a_0$. Even if we subtract the average of this charge density, the charge density remains very large at $r \sim 0.3a_0$. The corresponding Coulomb integral, $w_{dd} = 9$ eV, is then also large. Following the considerations in the Appendix, we replace \tilde{P}^0 by the sum $\sum_m \tilde{P}_{mm,mm}^0 \sim -1.4$ eV $^{-1}$ in our one-band model. It is immediately clear that local-field effects are very important, since $1 - w\tilde{P}^0 \sim 1 + 9 \times 1.4 \sim 14$. We can, however, see that the model is a bit too simple, since it overestimates the local-field effects, which in the full calculation “only” decrease the static dielectric function by a factor of 3. In our simple one-band model with only one $3d$ function, we obtain $\epsilon_{\text{LF}} = 10$ and $\epsilon_{\text{NLF}} = 118$. Below, we discuss a model which also includes the $4s$ electrons and which describes the local-field effects more accurately.

It is at this point interesting to discuss qualitatively why the dielectric function with local-field corrections is smaller than the one without these corrections. For simplicity, we consider $q \rightarrow 0$ and we assume that $f_\mu(q) = 1$. This is possible since $f_\mu(q \rightarrow 0) = 1/\sqrt{\Omega}$, if μ corre-

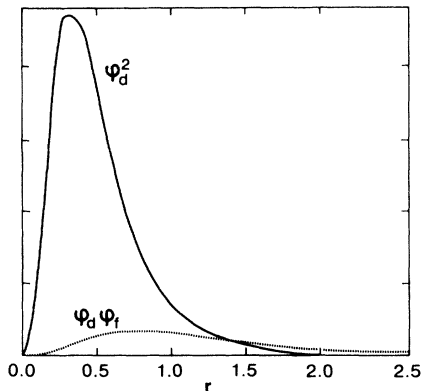


FIG. 4. The square $\phi_d^2(r)$ of the radial $3d$ function [$\int r^2 dr \phi_d^2(r) = 1$] as a function of r (full line). The dotted line shows the product $\phi_d(r)\phi_f(r)$.

sponds to equal functions. For simplicity we then put $\Omega = 1$ in the formulas below. Let us apply an external potential $V^{\text{ext}}e^{i\mathbf{q}\cdot\mathbf{r}}$ within the one-band model we have just discussed. In the $\mathbf{q} \rightarrow 0$ limit we then have $\tilde{P}^0(\mathbf{q}, 0) = -D(0)$, where $D(0)$ is the $3d$ density of states. Including local-field effects, we can then write

$$\tilde{V}^{\text{scr}}(\mathbf{q}, 0) = \tilde{V}^{\text{ext}}(\mathbf{q}, 0) - [v(q) + w(\mathbf{q})]D(0)\tilde{V}^{\text{scr}}(\mathbf{q}, 0). \quad (25)$$

We recall that according to the definition (10), the tilde over V^{scr} means that \tilde{V}^{scr} is not the \mathbf{q} th Fourier transform of $V^{\text{scr}}(\mathbf{r}, 0)$ but that it is the expectation value of $V^{\text{scr}}(\mathbf{r}, 0)$ taken between a Bloch sum of the localized functions. To see the origin of Eq. (25), we note that the potential \tilde{V}^{scr} leads to the induced charge density [see Eq. (14)] $-\tilde{B}(\mathbf{r})D(0)\tilde{V}^{\text{scr}}(\mathbf{q}, 0)$. Calculating the corresponding induced potential and taking the expectation value for the localized function Bloch sum leads to Eq. (25), if we use the result (19) for $\tilde{v}(\mathbf{q})$. Thus \tilde{V}^{scr} is the sum of the external potential and the induced potential, i.e., the potential from the induced charge acting back on the localized level. The potential acting back on the level has one part, $v(q)$, which is the $\mathbf{q} \rightarrow 0$ Fourier component and one part, $w(\mathbf{q})$, which contains the local-field corrections due to all the higher Fourier components induced by the inhomogeneity of the system. These potentials are schematically shown in Fig. 5. If we neglect the local-field effects, the magnitude of the induced potential is reduced for a given induced charge, since $w(\mathbf{q})$ is always positive [see Eq. (20)]. The reason is that when the local-field effects are neglected, only the $\mathbf{q} \rightarrow 0$ component is considered, which corresponds to smearing out the induced charge over the unit cell. In reality, the induced charge is built up by the localized level, and its interaction with this level is therefore stronger than if the charge had been smeared out. The relative effect is, however, moderate, since $w(\mathbf{q})$ approaches a constant as $\mathbf{q} \rightarrow 0$, while the term $v(q)$ diverges. Nevertheless, the local-field effects on the dielectric function can be large, even for $\mathbf{q} \rightarrow 0$, as shown below.

We can easily solve for \tilde{V}^{scr} from Eq. (25) and obtain

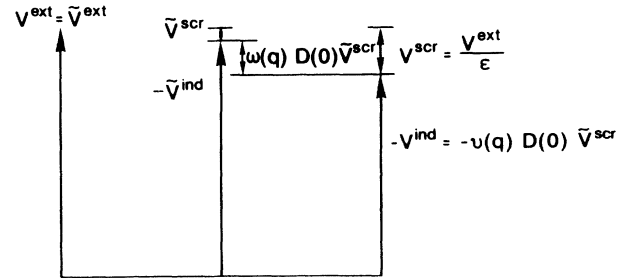


FIG. 5. The induced (\tilde{V}^{ind}) and screened (\tilde{V}^{scr}) potentials acting on the localized level and the corresponding Fourier components, V^{ind} and V^{scr} for the case when $f(\mathbf{q}) = 1$. The local-field effects are determined by $w(\mathbf{q})D(0) = |\tilde{V}^{\text{ind}} - V^{\text{ind}}|$, and the dielectric function is given by $\epsilon = V^{\text{ext}}/V^{\text{scr}}$.

$$\tilde{V}^{\text{scr}}(\mathbf{q}, 0) = \frac{\tilde{V}^{\text{ext}}(\mathbf{q}, 0)}{1 + [v(q) + w(\mathbf{q})]D(0)}. \quad (26)$$

To obtain the dielectric function, we now have to ask for the $\mathbf{q} \rightarrow 0$ Fourier component of the induced potential [second term on the right-hand side of Eq. (14)]

$$\begin{aligned} V^{\text{ind}}(\mathbf{q}, 0) &= -v(q)D(0)\tilde{V}^{\text{scr}}(\mathbf{q}, 0) \\ &= -\frac{v(q)D(0)}{1 + [v(q) + w(\mathbf{q})]D(0)}\tilde{V}^{\text{ext}}(\mathbf{q}, 0). \end{aligned} \quad (27)$$

We remind the reader that $\tilde{V}^{\text{ext}}(\mathbf{q}, 0) = V^{\text{ext}}(\mathbf{q}, 0)$, because we assume $f_\mu = 1$. Since we ask for the \mathbf{q} th Fourier component of the potential, the quantity $w(\mathbf{q})$ does not enter in the numerator, which is crucial for the result. As $\mathbf{q} \rightarrow 0$, the divergence of $v(q)$ leads to $V^{\text{ind}} \approx -V^{\text{ext}}$ (to leading order in $1/q^2$) and there is an efficient cancellation between the external and induced potential, implying that V^{scr} is small and the dielectric function is large. The cancellation is, however, not perfect, and the degree of cancellation can depend crucially on the local-field effects. In the example we have considered [$\mathbf{q} = (0.25, 0, 0)2\pi/a$] we find, for instance, that the induced potential is $-0.992V^{\text{ext}}$ and $-0.900V^{\text{ext}}$ without and with local-field effects, respectively. Although the difference in the induced potential is only 10% for this value of \mathbf{q} , the difference in cancellation, and in the dielectric function, is an order of magnitude. To see this formally, we write

$$\begin{aligned} \epsilon_{\text{LF}}(\mathbf{q}, 0) &= v(q)\{-\tilde{P}_{ss}^0 - \tilde{P}_{sd}^0 - \tilde{P}_{ds}^0 - \tilde{P}_{dd}^0 + (w_{ss} + w_{sd} + w_{ds} + w_{dd})(\tilde{P}_{ss}^0\tilde{P}_{dd}^0 - \tilde{P}_{sd}^0\tilde{P}_{ds}^0)\} \\ &\quad \times \{1 - w_{ss}\tilde{P}_{ss}^0 - w_{sd}\tilde{P}_{sd}^0 - w_{ds}\tilde{P}_{ds}^0 - w_{dd}\tilde{P}_{dd}^0 + (\tilde{P}_{ss}^0\tilde{P}_{dd}^0 - \tilde{P}_{sd}^0\tilde{P}_{ds}^0)(w_{ss}w_{dd} - w_{sd}w_{ds})\}^{-1}, \end{aligned} \quad (29)$$

where we have dropped the arguments \mathbf{q} and $\omega = 0$ of \tilde{P}^0 . Typical numbers are $w_{ss} = 0.1$ eV, $w_{sd} = w_{ds} = 0.5$ eV, $w_{dd} = 9$ eV, $\tilde{P}_{ss}^0 = -0.2$ eV $^{-1}$, $\tilde{P}_{sd}^0 = \tilde{P}_{ds}^0 = 0.3$ eV $^{-1}$, and $\tilde{P}_{dd}^0 = -1.4$ eV $^{-1}$. As above we have summed over the m quantum numbers for the \tilde{P}^0 involving $3d$ functions, e.g., $\tilde{P}_{sd}^0 = \sum_m \tilde{P}_{ss,mm}^0$. We can see that w_{dd} is much larger than the other Coulomb matrix elements. As before, we use $\mathbf{q} = (0.25, 0, 0)2\pi/a$, which leads to $v(q)/\Omega = 83$ eV. Inserting these numbers, we obtain $\epsilon_{\text{LF}} = 16$ and $\epsilon_{\text{NLF}} = 84$, in qualitative agreement with the full calculation ($\epsilon_{\text{LF}} = 23$ and $\epsilon_{\text{NLF}} = 68$). If we set $w_{ss} = w_{sd} = w_{ds} = 0$ we obtain

$$\epsilon_{\text{LF}} = v(q) \frac{-\tilde{P}_{ss}^0 - \tilde{P}_{sd}^0 - \tilde{P}_{ds}^0 - \tilde{P}_{dd}^0 + w_{dd}(\tilde{P}_{ss}^0\tilde{P}_{dd}^0 - \tilde{P}_{sd}^0\tilde{P}_{ds}^0)}{1 - w_{dd}\tilde{P}_{dd}^0}. \quad (30)$$

This leads to $\epsilon_{\text{LF}} = 17$, and the approximation of putting $w_{ss} = w_{sd} = w_{ds} = 0$ is apparently a good one. Finally we make the approximation that $w_{dd}|\tilde{P}_{dd}^0| \gg 1$. To leading order in $1/q^2$ we obtain

$$\begin{aligned} \epsilon_{\text{LF}} &= [1 - v(q)\tilde{P}_{ss}^0] + \left[1 - v(q)\frac{\tilde{P}_{dd}^0}{1 - w_{dd}\tilde{P}_{dd}^0}\right] \\ &\quad + v(q)\frac{-\tilde{P}_{ss}^0 - \tilde{P}_{sd}^0 - \tilde{P}_{ds}^0 - w_{dd}\tilde{P}_{sd}^0\tilde{P}_{ds}^0}{1 - w_{dd}\tilde{P}_{dd}^0}. \end{aligned} \quad (31)$$

The first bracket is the dielectric function ϵ_s due to $4s \rightarrow 4s$ transitions and it takes the value 18. The sec-

$$\begin{aligned} \epsilon(\mathbf{q}, 0) &= \frac{V^{\text{ext}}}{V^{\text{ind}} + V^{\text{ext}}} \\ &= \frac{1 + [v(q) + w(\mathbf{q})]D(0)}{1 + w(\mathbf{q})D(0)}. \end{aligned} \quad (28)$$

In the $\mathbf{q} \rightarrow 0$ limit, we can now neglect $w(\mathbf{q})$ in the numerator, but the factor $1 + w(\mathbf{q})D(0)$ in the denominator remains finite in this limit, and it may be important. We emphasize again that this effect results from the fact that $w(\mathbf{q})$ enters in the calculation of the potential \tilde{V}^{ind} felt by the localized level but not in V^{ind} entering in the dielectric function. This is illustrated in Fig. 5. If we neglected the term $w(\mathbf{q})D(0)$, there would be a small relative decrease in $|\tilde{V}^{\text{ind}}|$ and a large relative increase in \tilde{V}^{scr} . This would lead to a self-consistent readjustment, so that there were a small relative increase in the induced charge, until the value of \tilde{V}^{scr} were almost restored. Since $\tilde{V}^{\text{scr}} = V^{\text{scr}}$ when the local-field effects are neglected, the neglect of local-field effects then implies a large decrease of V^{scr} , which would become similar to \tilde{V}^{scr} in Fig. 5, and a large increase of the dielectric function $\epsilon = V^{\text{ext}}/V^{\text{scr}}$.

Since our one-band model does not give a very accurate description of the dielectric function with local-field corrections, we have also considered a two-band model. In this model we let the product functions $\tilde{B}_{\mathbf{q}\mu}$ in Eq. (5) stand for a product of two $3d$ functions and of two $4s$ functions. This leads to matrices of the dimension 2×2 and the matrix multiplications and inversions in Eq. (18) can be performed analytically. For simplicity, we consider $\mathbf{q} \rightarrow 0$ and we assume that $f_\mu(\mathbf{q}) = 1$ as above. Then we obtain to leading order in $1/q^2$

ond bracket is the dielectric function ϵ_d due to $3d \rightarrow 3d$ transitions with the value 10. The third term contains some cross terms with the value -8 . Since we have put $w_{ss} = 0$ we do not need to consider local-field corrections for ϵ_s . From the results in Eq. (31) we can see that ϵ_s and ϵ_d give comparable contributions. This may at first seem surprising, since we expect that the $3d$ electrons dominate the screening, due to the large $3d$ density of state. The denominator in the second bracket, describing the local-field effects for the $3d$ electrons, is, however, large ($=14$) and leads to a large reduction of the $3d \rightarrow 3d$ contribution, which becomes somewhat smaller than the $4s \rightarrow 4s$ contribution. This is completely different from

the case when local-field corrections are neglected. In that case the contribution from the $3d$ electrons alone is about seven times larger than the contribution from the $4s$ electrons alone. Finally, we notice that we obtain similar results if the product of two $4s$ functions is replaced by the product of two $4p$ functions. The important aspect is that both products provide an extended function, which is needed to describe the screening properties.

B. Loss function

We next consider the loss function in the limit when ω is finite and $\mathbf{q} \rightarrow 0$. For the imaginary part of the polarizability, there are then no contributions from the intraband transitions, since the energies of these transitions go to zero for $\mathbf{q} \rightarrow 0$. Let us consider the Fourier transformation of $P^0(\mathbf{r}, \mathbf{r}')$,

$$P^0(\mathbf{q}, \mathbf{q}, \omega) = \frac{1}{N\Omega} \int d^3r d^3r' e^{-i\mathbf{q}\cdot(\mathbf{r}-\mathbf{r}')} P^0(\mathbf{r}, \mathbf{r}', \omega), \quad (32)$$

which involves integrals $\int d^3r \psi_{\mathbf{k}n}^*(\mathbf{r}) e^{i\mathbf{q}\cdot\mathbf{r}} \psi_{\mathbf{k}-\mathbf{q}n'}$. For interband transitions $n \neq n'$ and $\mathbf{q} \rightarrow 0$, we expand $e^{i\mathbf{q}\cdot\mathbf{r}}$ as $1 + i\mathbf{q}\cdot\mathbf{r} + \dots$. From the orthogonality of the wave functions, it follows that there is no contribution from the first term. The dominating contribution then comes from the dipole transitions induced by $i\mathbf{q}\cdot\mathbf{r} + \dots$. This term effectively couples the occupied $3d$ functions to the unoccupied $4f$ functions, and the $3d \rightarrow 4f$ transitions should dominate the imaginary part of P^0 over the energy range of interest.

For the real part of P^0 the situation is somewhat more complex. Let us consider the dielectric function $\epsilon(\mathbf{q}, \mathbf{q}, \omega) = 1 - v(q)P^0(\mathbf{q}, \mathbf{q}, \omega)$ which fulfills the sum rule²⁴

$$\int_0^\infty \omega d\omega \text{Im}\epsilon(\mathbf{q}, \mathbf{q}, \omega) = \frac{2\pi^2 e^2 \rho}{m}, \quad (33)$$

where ρ is the density of electrons. We first consider the contributions from the intraband transitions. For energies much larger than the intraband transitions we have

$$\begin{aligned} \text{Re}\epsilon^{\text{Intra}}(\mathbf{q}, \mathbf{q}, \omega) &= 1 - \frac{2}{\pi\omega^2} \int_0^\infty \omega' d\omega' \\ &\times \text{Im}\epsilon^{\text{Intra}}(\mathbf{q}, \mathbf{q}, \omega'). \end{aligned} \quad (34)$$

Since the $\mathbf{q} \rightarrow 0$ intraband transitions take place just across the Fermi energy, it follows that

$$\int_0^\infty \omega' d\omega' \text{Im}\epsilon^{\text{Intra}}(\mathbf{q}, \mathbf{q}, \omega') \sim \sum_n \int_{\text{FS}} d^3k |\mathbf{v}_{\mathbf{k}n}|^2 \sim \omega_p^2, \quad (35)$$

where $\mathbf{v}_{\mathbf{k}n} \equiv \delta\epsilon(\mathbf{k}n)/\delta\mathbf{k}$ is the electron velocity of the state $\mathbf{k}n$, ω_p is the plasma frequency, and the integral is performed over the Fermi surface. For the $3d$ states, the

effective mass is large and the electron velocity is small. Therefore, the contribution from the intraband transitions to the sum rule Eq. (33) is small. For instance, by integrating to $\omega = 4.3$ eV, which includes the intraband and some of the interband transitions, only contributes about one electron per unit cell to the sum rule. Thus the $3d \rightarrow 3d$ intraband transitions play a rather small role for somewhat larger energies (> 5 eV) for the real part of the dielectric function. The remaining contribution must then come from interband transitions, which to a large extent are $3d \rightarrow 4f$ transitions. Furthermore, the real part of the dielectric function is rather small compared with the imaginary part for these energies (> 5 eV). Since the imaginary part is dominated by the interband transitions, we focus on the $3d \rightarrow 4f$ transitions below. While such a model is much too simple to describe the quantitative features of the loss function, it contains the qualitative features and in particular it explains why local-field effects are not very important.

We first consider the Coulomb integral w_{df} corresponding to the product function of $3d$ and $4f$ states. Since the $3d$ and $4f$ functions are orthogonal, the q th Fourier transform goes to zero for $q \rightarrow 0$. In this limit there is, therefore, no constant charge density to be subtracted away from the product. The product is, however, already rather small, as is illustrated in Fig. 4 by the dotted curve. Averaging over the 35 products of $3d$ and $4f$ functions, we find that the corresponding Coulomb integral is $w_{df} = 0.2$ eV. The smallness of this Coulomb integral is primarily due to the smallness of product of the radial orbitals $\phi_{3d}(r)\phi_{4f}(r)$, which follows from the fact that $\phi_{4f}(r)$ is small where $\phi_{3d}(r)$ is large and vice versa. This is in contrast to w_{dd} where by definition the two functions involved are large in the same parts of the space.

We now apply the one-band model in Eqs. (23) and (24) to the $3d \rightarrow 4f$ transition. Following the considerations in the Appendix, we add the diagonal matrix elements $\tilde{P}_{\mu\mu}^0$ for the 35 product functions. The result depends strongly on the ω and it increases with ω . For energies smaller than about 20 eV, the result is small and in the range 30–40 eV it is of the order 4 eV^{-1} . From Eq. (23) we then estimate that the local-field effects may change the loss function by a factor $1 + 0.2 \times 4 = 1.8$ in the range 30–40 eV. While this change is larger than the actually calculated one it is in qualitative agreement with the full calculations. In particular, we can see that the large difference between $w_{dd} = 9$ eV and $w_{df} = 0.2$ eV, is essential for understanding the large difference between the effects of the local-field corrections for the static dielectric function and the loss function.

Finally, we notice that there are large local-field effects in the region 60 to 80 eV. In this range there are transitions from the $3p$ core level to, in particular, $3d$ states. Since both the $3p$ and $3d$ levels are well localized, we may expect the corresponding integral $w_{pd}(\mathbf{q})$ to be relatively large. The joint density of states should also be large, due to the sharpness of the $3p$ level and the narrowness of the $3d$ density of states. From this one would expect large local-field effects from the $3p$ core transitions, as is also observed.

VI. XC LOCAL-FIELD EFFECTS

In the previous sections, we have focused on the local-field effects due to the inhomogeneity of the system. Here we discuss the XC local-field effects due to exchange-correlation effects.²⁵ Thus we consider the effective potential V^{eff} in the density functional formalism,⁴ which has an exchange-correlation contribution v_{xc} , in addition to the Hartree potential discussed above. We here have the local density approximation for v_{xc} in mind, and in the explicit calculations we, for simplicity, only consider the exchange part, since it is much larger than the correlation part. Equation (9) is then generalized as

$$V^{\text{eff}}(\mathbf{r}, \omega) = V^{\text{ext}}(\mathbf{r}, \omega) + \int d^3r' \int d^3r'' v(\mathbf{r} - \mathbf{r}') \times P^0(\mathbf{r}', \mathbf{r}'', \omega) V^{\text{eff}}(\mathbf{r}'', \omega) + \frac{\delta v_{\text{xc}}(\mathbf{r})}{\delta \rho(\mathbf{r})} \int d^3r'' P^0(\mathbf{r}, \mathbf{r}'', \omega) V^{\text{eff}}(\mathbf{r}'', \omega). \quad (36)$$

Introducing the quantity

$$I_{\mu\nu}^{\text{xc}}(\mathbf{q}) = \int d^3r \tilde{B}_{\mathbf{q}\mu}^*(\mathbf{r}) \frac{\delta v_{\text{xc}}(\mathbf{r})}{\delta \rho(\mathbf{r})} \tilde{B}_{\mathbf{q}\nu}(\mathbf{r}) \quad (37)$$

we obtain the generalization of Eq. (18)

$$\epsilon_{\text{LF}}^{-1}(\mathbf{q}, \omega) = 1 + v(\mathbf{q}) \sum_{\mu\nu} f_{\mu}(\mathbf{q}) \{ \tilde{P}^0 [1 - (\tilde{v} + \tilde{I}^{\text{xc}}) \tilde{P}^0]^{-1} \}_{\mu\nu} \times f_{\nu}^*(\mathbf{q}). \quad (38)$$

The local-field effects due to the exchange-correlation effects are then determined by \tilde{I}^{xc} and the local-field effects due to the inhomogeneity are determined by w , as before.

It is then interesting to ask for the relative importance of the two types of local-field effects. For diamond it has been found that the two effects are of similar magnitude but of opposite sign,²⁶ and it has been argued that for this type of system there may be a substantial cancellation between the two types of effects.²² Here we want to address if there may also be such a cancellation for systems with localized levels, like Ni and NiO.

We assume that the localized 3d orbital can be described by a Slater orbital

$$\phi(r) = A r^2 e^{-r/\lambda}, \quad (39)$$

where A is a normalization constant. Using this orbital we calculate $\tilde{I}_{3d3d,3d3d}^{\text{xc}}$ and $w_{3d3d,3d3d}$, and compare their magnitude. If we only include the contribution from the N_{3d} occupied 3d orbitals, the spherical average of the density is given by

$$\rho(r) = N_{3d} \phi^2(r). \quad (40)$$

We only consider the exchange potential $v_{\text{x}} \sim \rho^{1/3}$, for which we have that

$$\frac{\delta v_{\text{x}}}{\delta \rho} = \frac{4}{9} \frac{\varepsilon_{\text{x}}}{\rho} \quad (41)$$

where ε_{x} is the exchange energy per electron of a homo-

geneous system. We then have

$$\tilde{I}_{3d3d,3d3d}^{\text{xc}} = \int d^3r \phi^4(r) \frac{\delta v_{\text{x}}}{\delta \rho} = \frac{4}{9N_{3d}} \int d^3r \phi^2(r) \varepsilon_{\text{x}}. \quad (42)$$

In Eq. (41) the total density enters, and the value of $\delta v_{\text{x}}/\delta \rho$ and thereby also \tilde{I}^{xc} would be further reduced if we considered the core electrons. The integral should be performed over the Wigner-Seitz sphere, but since the Slater orbital has little weight outside the Wigner-Seitz sphere for values of λ appropriate for the late 3d elements, we have extended the integral to infinity. We then find

$$\tilde{I}_{3d3d,3d3d}^{\text{xc}} = -0.079 \frac{1}{\lambda N_{3d}^{2/3}} \text{Ry}. \quad (43)$$

In the same approximation we find

$$\tilde{w}_{3d3d,3d3d} = \frac{0.516}{\lambda} + \frac{12}{5R_{\text{WS}}} - \frac{4}{R_{\text{WS}}} \left(\frac{3}{2} - \frac{7\lambda^2}{R_{\text{WS}}^2} \right) \text{Ry}, \quad (44)$$

where R_{WS} is the Wigner-Seitz radius. Here the first term comes from the Coulomb integral of $\phi^2(r)$ and the second and third terms are due to the correction from subtracting the average charge from $\phi^2(r)$. To reproduce the value of the Coulomb integral of the true 3d orbital, we have to put $\lambda = 0.266$. Using $R_{\text{WS}} = 2.6 a_0$, we then obtain $w = 1.94 + 0.92 - 2.20 = 0.66 \text{ Ry}$ and $\tilde{I}^{\text{xc}} = 0.07 \text{ Ry}$.

For the Ni 3d orbitals, we, therefore, find that the local-field effects due to the inhomogeneities are about an order of magnitude larger than the XC local-field effects. In the limit when $\lambda/R_{\text{WS}} \ll 1$, we can see from Eqs. (43) and (44) that both w and \tilde{I}^{xc} scale as $1/\lambda$, and the relative importance of the two types of local-field effects is independent of the extent λ of the orbital. This follows because the last two terms in Eq. (44) then can be neglected. Already for the Ni 3d orbital, these terms are, however, not negligible, and as λ/R_{WS} grows larger, these terms become important. For instance, for $\lambda = 0.4$ we find that $w = 0.15 \text{ Ry}$ and $\tilde{I}^{\text{xc}} = 0.04 \text{ Ry}$, and the XC local-field effects are not negligible any more. We conclude that for diamond the XC local-field effects are more important both because the 2s and 2p orbitals are more extended (λ larger) and because the number of electrons N_{3d} is smaller. Thus it is not surprising that the two types of local-field effects were found to be of comparable magnitude for diamond.²⁶

VII. SUMMARY

We have presented theoretical results for the dielectric function within RPA for NiO and Ni and experimental results for the loss function for NiO. Comparison between theory and experiment shows that theory reproduces the loss function of NiO fairly well. We have discussed the local-field effects extensively and shown that these are important for the static dielectric function but not very important for the loss function. We find that the im-

portance of the local-field effects is related to the magnitude of the Coulomb interaction w for a charge density obtained from a product between the wave functions involved in the most important transitions minus the average of this product density. We have shown that the loss function is primarily related to $3d \rightarrow 4f$ transitions while the static dielectric function is mainly determined by the $3d \rightarrow 3d$ intraband transitions. Since $w_{df} \sim 0.2$ eV is much smaller than $w_{dd} \sim 9$ eV, we can understand the difference between the importance of local-field effects for the loss function and the static dielectric function. We have further illustrated why the local-field effects reduce the static dielectric function. We found that this reduction is so efficient for $3d \rightarrow 3d$ contribution that the $4s \rightarrow 4s$ contribution becomes important for Ni, although the $4s$ density of states is much smaller than the $3d$ density of states.

ACKNOWLEDGMENTS

We want to thank I. I. Mazin for stimulating and helpful discussions. This work has been supported in part by the European Community program Human Capital and Mobility through Contract No. CHRX-CT93-0337.

APPENDIX

In this appendix, we discuss how a model with a degenerate orbital can be approximated by a model with

$$(1 - \tilde{v}\tilde{P}^0)^{-1} = \frac{1}{1 - 3v_0p_0} \begin{pmatrix} 1 - 2v_0p_0 & v_0p_0 & v_0p_0 & 0 & 0 & 0 \\ v_0p_0 & 1 - 2v_0p_0 & v_0p_0 & 0 & 0 & 0 \\ v_0p_0 & v_0p_0 & 1 - 2v_0p_0 & 0 & 0 & 0 \\ 0 & 0 & 0 & 1 & 0 & 0 \\ 0 & 0 & 0 & 0 & 1 & 0 \\ 0 & 0 & 0 & 0 & 0 & 1 \end{pmatrix}. \quad (\text{A4})$$

Calculating $\tilde{P}^0(1 - \tilde{v}\tilde{P}^0)^{-1}$ and performing the sum over μ and ν in Eq. (18), we obtain

$$\sum_{\mu\nu} f_\mu \{ \tilde{P}^0(1 - \tilde{v}\tilde{P}^0)^{-1} \}_{\mu\nu} f_\nu = \frac{3p_0}{1 - 3v_0p_0}. \quad (\text{A5})$$

This equation shows that within this model we can replace the threefold degenerate orbital by a nondegenerate

orbital. To simplify the notation, we consider the case with a threefold degenerate p orbital. The generalization to any other degeneracy is straightforward. We first form the six product functions $B_{\mathbf{q}iLL'}$, where the atomic index i only takes one value and L and L' can each take three values with the restriction $L \leq L'$. The product functions are labeled so that the first three ones correspond to $L = L'$ and the following three correspond to $L < L'$. From the normalization, it then follows that the first three product functions integrate to $1/\Omega$, where Ω is the volume of the unit cell and the following three to zero. For simplicity we put $\Omega = 1$ and write

$$f_\mu(\mathbf{q} \rightarrow 0) = \begin{cases} 1 & \text{for } \mu \leq 3 \\ 0 & \text{for } \mu > 3. \end{cases} \quad (\text{A1})$$

For the Coulomb integrals we then make the assumption that

$$\tilde{v}_{\mu\nu}(\mathbf{q}) = \begin{cases} v_0 & \text{for } \mu, \nu \leq 3 \\ 0 & \text{for } \mu \text{ or } \nu > 3, \end{cases} \quad (\text{A2})$$

since the dominating interaction is a monopole interaction for both $\mu \leq 3$ and $\nu \leq 3$, and a multipole interaction for $\mu > 3$ or $\nu > 3$. We also assume that the polarizability matrix is diagonal

$$\tilde{P}^0_{\mu\nu} = \begin{cases} p_0\delta_{\mu\nu} & \text{for } \mu \leq 3 \\ 2p_0\delta_{\mu\nu} & \text{for } \mu > 3, \end{cases} \quad (\text{A3})$$

since the nondiagonal elements are found to be much smaller, as one would expect from Eq. (7). Corresponding to the basis function $L < L'$ there is also a second contribution to \tilde{P}^0 from $L > L'$, which is included by using the factor 2 in Eq. (A3) for $\mu > 3$. We then perform the matrix operations in Eq. (18) and find

orbital, if we replace the polarizability by the sum of the polarizability over the three components $L = L'$. The same immediately follows for more general cases. We observe, however, that the result is rather sensitive to the assumption (A2) of all $\tilde{v}_{\mu\nu}$ being equal (for μ and ν corresponding to $L = L'$), and that we should only expect a qualitative agreement with the full calculation when the assumptions (A2) and (A3) are not fulfilled.

¹ N.F. Mott, Proc. Phys. Soc. London Sect. A **62**, 416 (1949).

² A. Fujimori, F. Minami, and S. Sugano, Phys. Rev. B **29**, 5225 (1984); A. Fujimori and F. Minami, *ibid.* **30**, 957 (1984).

³ G.A. Sawatzky and J.W. Allen, Phys. Rev. Lett. **53**, 2339 (1984).

⁴ P. Hohenberg and W. Kohn, Phys. Rev. **136**, B864 (1964); W. Kohn and L.J. Sham, *ibid.* **140**, A1133 (1965); for a review see, e.g., R.O. Jones and O. Gunnarsson, Rev. Mod. Phys. **61**, 689 (1989).

⁵ K. Terakura, A.R. Williams, T. Oguchi, and J. Kübler, Phys. Rev. Lett. **52**, 1830 (1984).

- ⁶ S. Hüfner, J. Osterwalder, T. Riesterer, and F. Hullinger, *Solid State Commun.* **52**, 793 (1984).
- ⁷ H. Ehrenreich and M.H. Cohen, *Phys. Rev.* **115**, 786 (1959).
- ⁸ S.L. Adler, *Phys. Rev.* **126**, 413 (1962).
- ⁹ N. Wiser, *Phys. Rev.* **129**, 62 (1963).
- ¹⁰ L. Hedin, *Phys. Rev.* **139**, A796 (1963).
- ¹¹ F. Aryasetiawan, *Phys. Rev. B* **46**, 13 051 (1992).
- ¹² F. Aryasetiawan, U. von Barth, P. Blaha, and K. Schwarz (unpublished).
- ¹³ S.G. Louie, J.R. Chelikowsky, and M.L. Cohen, *Phys. Rev. Lett.* **34**, 155 (1975).
- ¹⁴ F. Aryasetiawan and O. Gunnarsson, *Phys. Rev. B* **49**, 7219 (1994).
- ¹⁵ O.K. Andersen, *Phys. Rev. B* **12**, 3060 (1975); O.K. Andersen and O. Jepsen, *Phys. Rev. Lett.* **53**, 2571 (1984).
- ¹⁶ L.J. Sham, *Phys. Rev. B* **6**, 3584 (1972); W. Hanke, *ibid.* **8**, 4585 (1973); W. Hanke and L.J. Sham, *ibid.* **12** 4501 (1975).
- ¹⁷ F. Aryasetiawan and O. Gunnarsson, *Phys. Rev. B* **49**, 16 214 (1994).
- ¹⁸ E. Hayashi and M. Shimizu, *J. Phys. Jpn.* **26**, 1396 (1969); S.K. Sinha, *Phys. Rev.* **177**, 1256 (1969).
- ¹⁹ A. Svane and O.K. Andersen, *Phys. Rev. B* **34**, 5512 (1986).
- ²⁰ J. Fink, *Adv. Electron. Electron Phys.* **75**, 121 (1989).
- ²¹ J. Daniels, C. von Festenberg, H. Raeter, and K. Zepfenfeld, in *Springer Tracts in Modern Physics* (Springer-Verlag, Berlin, 1970), Vol. 54, p. 77.
- ²² I.I. Mazin, E.G. Maksimov, S.N. Rashkeev, and Yu. A. Uspenskii, *Zh. Eksp. Teor. Fiz.* **90**, 1092 (1986) [*Sov. Phys. JETP* **63**, 637 (1986)].
- ²³ L.A. Feldcamp, M.B. Stearns, and S.S. Shinozaki, *Phys. Rev. B* **20**, 1310 (1979).
- ²⁴ P. Nozières and D. Pines, *Phys. Rev.* **109**, 741 (1958).
- ²⁵ L. Hedin and B.I. Lundqvist, *J. Phys. C* **4**, 2064 (1971).
- ²⁶ M.S. Hybertsen and S.G. Louie, *Phys. Rev. B* **35**, 5585 (1987).